Compositional variation of laurite at Union Section in the Western Bushveld Complex

W.D. Maier
Department of Geology, University of Pretoria, Pretoria, 0002 Republic of South Africa
Email: wdmaier@scientia.up.ac.za

H.M. Prichard
Department of Earth Sciences, Cardiff University, P.O. Box 914, Cardiff, Wales
E-mail: sglhmp@cardiff.ac.uk

S.-J. Barnes
CERM, Université du Québec, Chicoutimi, G7H 2B1, Canada
E-mail: sjbarnes@uqac.uquebec.ca

P.C. Fisher
Department of Earth Sciences, Cardiff University, P.O. Box 914, Cardiff, Wales
E-mail: FisherPC@cardiff.ac.uk

Accepted 25th February 1999

Abstract — One hundred and forty five grains of laurite in polished sections of samples from one borehole through the major chromitite layers and some chromite-bearing silicate rocks of the Lower and Critical Zones of the western Bushveld Complex at Union Section have been located and analysed by scanning electron microscope. Ninety per cent by number of laurite grains are included within chromite, with the remainder being located on chromite–silicate grain boundaries, and in interstitial silicates and sulphides. The composition of laurite shows considerable variation within individual samples. Furthermore, there is no apparent correlation between whole-rock Ru and Cr contents in our samples, arguing against a model whereby laurite exsolved from the chromite lattice. Based on a well-defined correlation between whole-rock S, PPGE (Rh+Pt+Pd), and IPGE (Os+Ir+Ru) contents, we favour a mechanism whereby laurite crystallized from segregating sulphide melt and was subsequently entrapped by growing chromite grains.

Introduction

In addition to the strongly chalcophile character of the PGE, [$D_{sulph\ melt/sil\ melt}$ between 10^3 and 10^6 (Stone *et al.*, 1990; Fleet *et al.*, 1991; Bezmen *et al.*, 1994)], the enrichment of IPGE (Os + Ir + Ru) over PPGE (Pd + Pt + Rh) in many sulphide-poor mafic and ultramafic rocks suggests that the PGE may behave as compatible elements in the presence of chromite and olivine (Barnes *et al.*, 1988, and references therein). Chromite in chromitite and silicate rocks from layered intrusions and ophiolites commonly contains inclusions of laurite ($RuOsIrS_2$). Thus, the origin of laurite may bear directly on the origin of the PGE mineralization. In spite of the fact that laurite is an ubiquitous phase in chromite of the Lower and Critical Zones of the Bushveld Complex, no systematic study of laurite compositions throughout the Complex has been attempted. Here, we present analyses of all laurite grains we located in the Lower, Middle, and Upper Group (LG, MG, and UG) Chromitites, chromitite stringers associated with the Tarentaal, Merensky, and Bastard Reefs, and some chromite-bearing silicate rocks from a borehole sequence through the Lower and Critical Zones of the western Bushveld Complex at Union Section. The reader is referred to Maier *et al.* (1996) for a lithological description of the sequence analysed as well as sampling localities and stratigraphic positions of the NG samples (Table 1). The sampling locality, stratigraphic position and lithology of the U-samples (Table 1) is described in Eales and Reynolds (1986). By means of our database, we evaluate the main models generally invoked in the origin of laurite inclusions in chromite.

Analytical methods

The laurite grains were located using the 4QBSD on a Cambridge Instruments S360 Scanning Electron Microscope at the University of Cardiff. They were analysed using the attached Oxford Instruments AN10 EDX analyser. Operating conditions for quantitative analyses were an EHT of 20 kv, a specimen calibration current of approximately 1 nA, and a working distance of 25 mm. After every four analyses, the cobalt standard was reanalysed, in order to check for any drift in the analytical conditions.

Results

The compositions of the laurite grains are listed in Table 1. Almost all the laurite grains identified in this study are included in chromite grains (91% by number of 145 grains analysed). Seven per cent of grains are located on chromite–silicate grain boundaries, 1.5% are hosted by interstitial silicates, and 1 laurite grain (<1% of grains analysed) by base-metal sulphides. In the studied UG2 samples, 100% of laurite grains are included in chromite. The results are in broad accord with the data of Merkle (1992), who observed that 80% of laurites between the MG1 and the UG1 occur as inclusions in chromite. Approximately 50% of the laurite inclusions in chromite occur in isolation, with the remainder being associated with inclusions of silicates, rutile, BMS (mainly chalcopyrite, pentlandite, and lesser millerite, pyrrhotite, and pyrite), and other PGM (Pt–Pd sulphides, Pt–Cu–Rh sulphides, alloys, arsenides, and tellurides). Notably, where laurite occurs together with other PGM, it is always the largest grain.

Table 1 Composition of laurites in the Lower and Critical Zones of the Bushveld Complex (in wt.%)

Sample	Rock type	Mineral association	Size (mμ)	S	Ru	Os	Ir	Cr	Fe	Ni	Cu	Total	Other	Host phase cr	gb	bms	sil
U 235/2	Merensky top-chromitite	Cpy PtS PtFe Sil	35.0x17.0	38.88	49.74	2.10	3.57	0.15	2.57	1.02	nd	98.01		X			
U 235/8E	UG2-30cm above base	Cr	4.5x3.6	36.69	51.81	5.09	2.12	1.45	1.04	nd	nd	98.20		X			
		Cr Rut.	3.0x3.0	37.16	51.21	7.37	2.70	1.04	0.94	nd	nd	100.42		X			
		Cr Rut.	5.8x3.5	37.16	53.08	5.55	2.80	1.22	0.87	nd	nd	100.69		X			
		Cr	7.0x3.2	36.41	52.01	4.86	2.34	1.58	0.96	nd	nd	98.13		X			
		Cr Sil.	5.6x4.0	37.45	52.59	5.58	2.27	1.26	0.80	nd	nd	99.94		X			
		Cr Sil. Rut.	6.7x4.6	36.99	52.20	4.77	3.45	1.06	0.73	nd	nd	99.20		X			
		Cr Rut.	3.3x2.6	36.49	50.66	5.96	2.74	1.69	1.30	nd	nd	98.83		X			
		Cr Rut.	3.1x2.4	34.07	48.26	5.73	2.72	1.71	0.94	nd	nd	93.43	Ti 3.85%	X			
		Cr	5.6x4.8	36.39	50.44	7.19	3.37	1.57	0.92	nd	nd	99.88		X			
		Cr Rut.	3.4x2.8	35.43	50.26	5.12	2.81	1.63	1.18	nd	nd	96.44	Ti 1.96%	X			
		Cr Rut. Sil.	4.0x4.0	36.43	51.21	6.01	2.56	1.59	1.24	nd	nd	99.05		X			
		Cr Rut. Sil.	4.7x4.6	36.76	50.57	8.02	2.75	1.58	1.11	nd	nd	100.79		X			
		Cr Cpy.	4.8x4.7	37.06	53.80	3.63	3.09	1.28	1.07	nd	nd	99.93		X			
		Cr	4.5x2.3	35.82	51.97	5.48	3.14	1.71	1.09	nd	nd	99.21		X			
		Cr Rut. Sil.	4.8x2.8	37.09	54.34	5.42	2.47	1.38	0.98	nd	nd	101.67		X			
		Cr	4.7x3.8	36.68	51.24	6.16	2.36	1.45	0.97	nd	0.36	99.21		X			
U 235/8D	UG2-20cm above base	Cr Sil. Ca phase?	6.4x5.9	37.35	54.63	3.80	2.99	1.16	0.78	nd	nd	100.71		X			
		Cr Rut.	2.4x2.3	36.24	51.47	6.12	2.83	1.97	1.34	nd	nd	99.98		X			
		Cr	3.7x3.4	37.36	53.05	3.82	4.03	1.64	1.22	nd	nd	101.12		X			
		Cr Rut. Sil.	4.0x3.6	36.12	56.84	1.86	1.36	1.45	1.03	nd	nd	100.45		X			
		Cr Rut. Sil.	5.0x3.6	37.51	52.12	5.82	1.70	1.28	0.88	nd	nd	99.31		X			
		Cr Rut.	6.2x5.5	37.78	54.85	4.23	2.98	1.25	0.86	nd	nd	101.95		X			
		Cr	2.6x2.0	35.73	51.61	6.70	3.19	2.50	1.41	nd	nd	101.13		X			
		Cr	5.8x3.6	36.57	48.27	10.21	2.88	1.43	1.18	nd	nd	100.55		X			
		Cr Cpy. Rut.	4.6x3.5	37.85	54.66	4.48	1.87	1.34	0.94	nd	nd	101.12		X			
		Cr	9.2x3.5	37.21	53.98	4.45	1.35	1.30	0.94	nd	nd	99.22		X			
		Cr Sil.	3.0x2.3	35.98	48.75	7.48	4.83	2.11	1.26	nd	nd	100.40		X			
		Cr Sil.	5.3x2.5	36.40	51.88	4.75	0.82	1.56	1.10	nd	nd	96.50		X			
		Cr Rut. Sil.	3.9x3.3	37.17	54.86	2.06	1.20	1.51	0.99	nd	nd	97.58		X			
U 212/2	UG1	Cr Rut. Sil.	3.5x2.7	36.68	51.05	7.91	2.19	1.73	1.03	nd	nd	100.59		X			
		Cr	6.7x6.6	36.55	50.41	7.68	2.20	1.40	0.80	nd	nd	99.04		X			
		Cr IrPtOsRhRu	7.2x6.5	37.42	55.30	1.66	3.25	1.03	0.53	nd	nd	99.20		X			
		Cr	2.0x2.0	36.51	55.66	0.19	1.53	2.42	1.51	nd	nd	97.82		X			
		Cr Rut. Sil.	3.0x2.0	34.37	51.74	3.15	1.71	4.10	2.33	nd	nd	97.39		X			
		Cr IrOs Sil.	6.3x3.7	38.10	56.69	1.45	3.87	1.26	0.66	nd	nd	102.03		X			
		Cr	2.8x2.2	37.12	57.34	1.75	1.16	2.15	1.31	nd	nd	100.82		X			
		Cr	2.4x2.0	37.04	56.51	0.62	2.50	1.89	1.29	nd	nd	99.85		X			
		Cr	2.2x2.1	35.48	50.58	6.67	2.51	1.94	1.13	nd	nd	98.31		X			
		Cr crack	3.2x2.9	37.98	57.19	1.53	2.42	1.40	0.84	nd	nd	101.36			X		
		Cr	2.7x2.3	35.99	52.58	5.14	2.02	2.54	1.58	nd	nd	99.85		X			
NG3 152.6	MG4b	Cr	4.7x4.1	37.01	51.50	7.05	3.38	1.39	0.94	nd	nd	101.27		X			
		Cr	2.8x2.5	36.18	50.06	5.76	3.95	1.67	1.29	nd	nd	98.91		X			
		Cr cpy	5.5x4.4	36.20	48.01	7.87	3.80	1.53	1.11	nd	nd	98.52		X			
		Cr	3.5x2.8	36.59	49.09	7.34	4.59	1.48	1.21	nd	nd	100.30		X			
NG3 155.85	MG4a	Cr PtS Rut.	3.0x2.7	35.70	46.34	7.60	6.09	1.57	1.45	nd	nd	98.74		X			
		Cr Spin. Pent.	4.5x3.2	34.65	45.91	8.72	3.32	1.26	1.81	nd	nd	95.47		X			
		Cr Rut.	2.1x2.0	34.60	48.68	7.22	3.14	1.78	2.58	nd	nd	97.99	Ti 1.3 %	X			
		Cr IrAs?	3.1x3.0	35.53	45.56	11.71	4.25	1.54	1.19	nd	nd	99.77		X			
NG3 211.45b	MG3	Cr Cpy. Rut.	3.2x3.0	36.36	46.06	7.30	4.43	2.05	1.62	nd	nd	97.84		X			
		Cr	3.5x3.5	35.95	47.24	8.25	3.99	1.45	1.22	nd	nd	98.10		X			
		Cr	2.8x2.7	35.35	48.46	6.97	4.78	1.47	1.77	nd	nd	98.80		X			
		Cr PtPdS Cpy.	2.7x2.4	36.46	47.03	6.87	3.62	1.66	1.83	0.31	nd	97.77	Ti 1.55%	X			
		Cr Pt?	4.2x4.0	36.52	47.92	9.84	3.90	1.23	1.57	nd	nd	100.98		X			
NG3 219.42	MG2	Cr	2.4x2.4	35.96	48.62	7.11	3.86	2.22	1.59	nd	nd	99.36		X			
		Cr PtPdS	2.0x1.7	34.92	44.29	8.44	3.28	2.21	2.13	0.56	nd	95.84		X			
		Cr	3.1x3.0	37.30	48.66	8.58	3.17	1.76	1.62	0.28	nd	100.38		X			
NG1 65.6	chromite in pyroxenite	Cr	2.8x2.2	37.23	52.55	5.55	4.71	2.33	1.40	nd	nd	103.78		X			
		Cr Rut. Pt	3.1x2.7	36.38	49.48	6.72	3.09	1.82	1.27	nd	nd	98.74		X			
		Cr	3.1x2.7	36.37	49.85	7.14	3.70	1.85	1.38	nd	nd	99.90		X			
		Cr Rut.	4.2x3.6	36.57	50.54	6.93	2.75	1.81	1.23	nd	nd	99.82		X			
		Cr PtRhS Cpy.	11.0x9.3	36.99	46.78	10.03	1.69	0.83	0.58	nd	nd	96.90		x			
		Cr	2.9x2.4	36.64	49.60	7.66	4.92	2.02	1.23	nd	nd	102.07		X			
		Cr PtPdS	3.2x2.4	36.65	48.43	7.59	3.21	2.29	1.50	nd	nd	99.86		X			
		Cr	3.4x2.8	37.08	46.27	5.81	4.71	1.97	1.16	0.32	nd	97.32		X			
		Cr PtS Rut	3.7x2.9	37.45	50.70	6.14	3.81	1.65	1.41	nd	nd	101.15		X			
		Cr	3.1x2.4	36.86	50.49	6.75	3.91	1.77	1.35	nd	nd	101.13		X			
		Cr CuS? Pt?	2.8x2.4	36.47	44.56	8.83	4.75	2.12	2.37	0.34	0.37	99.81		X			
		Cr RhIrAs PtS	5.2x2.1	36.72	47.52	6.50	3.41	2.65	2.36	0.50	nd	99.66		X			
		Cr	2.1x2.1	36.12	50.46	5.84	3.58	2.20	1.28	nd	nd	99.49		X			
		Cr PtPdS Rut.	3.6x3.2	36.79	46.97	6.09	4.43	1.77	1.50	nd	nd	97.54		X			
		Cr PtRhIrS PtS	3.4x2.8	35.72	44.83	5.18	6.43	1.91	0.90	nd	nd	94.98	Pt 1.96%	X			
		Cr	2.5x2.0	36.33	49.49	8.48	3.80	2.22	1.45	nd	nd	99.76		X			
		Cr PtPdS Rut.	4.2x4.0	37.58	47.17	6.78	3.89	1.72	1.28	nd	nd	98.42		X			

Table 1 (Continued) Composition of laurites in the Lower and Critical Zones of the Bushveld Complex (in wt.%)

Sample	Rock type	Mineral association	Size (mμ)	S	Ru	Os	Ir	Cr	Fe	Ni	Cu	Total	Other	Host phase cr	gb	bms	sil
NG1 90.33	chromite in pyroxenite	Cr	4.7x2.8	36.60	50.73	8.72	1.76	1.39	1.22	nd	nd	100.42		X			
		Cr Pent.	5.2x4.2	37.25	49.39	7.70	4.89	1.23	1.41	0.60	nd	102.47			X		
		Cr Pent. PtPdS	7.6x6.8	37.08	47.41	5.61	6.48	0.96	1.14	nd	nd	98.67	Pt 1%	X			
		Cr Cpy?	2.1x2.2	32.14	37.85	5.42	5.63	4.49	5.00	0.99	2.89	94.40	Pt 2.5%	X			
		Cr	2.3x2.0	35.36	45.01	8.50	4.55	1.94	1.64	nd	nd	97.19		X			
		Cr	7.8x4.5	36.84	48.37	8.14	4.72	1.20	1.12	nd	nd	98.39		X			
		Cr	7.6x4.6	36.51	46.77	8.76	5.08	1.23	1.17	nd	nd	97.53		X			
NG1 152.5	LG7	Cr	2.6x2.5	35.56	47.15	11.70	3.03	2.11	1.63	nd	nd	101.18		X			
		Cr	4.1x2.7	34.50	47.82	8.40	2.35	2.92	2.31	nd	nd	98.30			X		
		Cr	4.8x3.6	35.81	45.58	12.09	3.37	1.25	0.99	nd	nd	99.10		X			
NG1 242.43A	LG5a	Cr	5.0x3.7	36.51	51.65	6.10	3.10	1.44	0.82	nd	nd	99.62		X			
		Cr Rut.	3.0x2.5	36.64	50.38	9.03	3.32	2.08	1.42	nd	nd	102.85		X			
		Cr	6.5x4.6	37.39	49.10	7.84	6.69	1.60	0.91	nd	nd	103.52		X			
		Cr	5.7x2.0	34.71	47.90	7.54	4.44	2.70	1.54	nd	nd	98.82		X			
		Cr	2.6x2.1	33.58	46.07	7.52	5.10	3.72	2.34	nd	nd	98.33		X			
		Cr	3.1x2.8	36.95	50.35	8.58	4.50	1.56	1.07	nd	nd	103.11		X			
NG1 245.4A	chromite in pyroxenite	Cr	27.0x18.0	36.12	48.40	7.20	3.14	0.66	0.54	nd	nd	96.06			X		
		Cr PtPdS	7.2x6.0	36.17	47.98	6.27	5.21	1.44	1.01	nd	nd	98.08		X			
		Cr Pent. PtS	12.4x8.0	36.62	48.30	6.70	4.62	1.14	0.68	nd	nd	98.06		X			
		Cr	6.1x3.8	36.14	48.34	7.40	3.58	1.35	0.86	nd	nd	97.68		X			
		Cr IrOs	2.5x2.3	33.12	42.32	10.80	6.00	2.43	1.19	nd	nd	95.85		X			
		Cr Sil.	5.6x5.2	36.79	49.18	7.12	4.69	1.33	1.01	nd	nd	100.12			X		
		Cr	12.0x7.5	36.83	48.56	5.91	4.27	0.78	0.77	nd	nd	98.13			X		
		Cr	9.3x3.8	36.98	47.96	7.11	4.35	1.19	0.78	nd	nd	98.37			X		
		Cr Sil.	7.0x4.3	37.06	49.90	7.42	4.82	1.32	0.98	nd	nd	101.50			X		
		Cr	6.8x6.5	36.70	50.92	6.08	4.35	1.25	0.50	nd	nd	99.80		X			
		Cr	5.1x4.4	36.66	49.48	7.26	4.69	1.61	1.09	nd	nd	100.80		X			
		Cr Sil.	3.9x2.1	34.81	48.86	6.82	3.52	1.81	1.24	nd	nd	97.07	Ti 0.23%		X		
		Cr	5.7x4.2	36.21	48.46	7.76	4.13	1.27	0.72	nd	nd	98.54		X			
		Cr	2.7x2.0	35.65	48.01	6.31	3.93	1.94	1.38	nd	nd	97.21		X			
		Cr	6.6x6.4	35.45	47.56	6.93	5.00	2.34	1.55	nd	nd	98.84			X		
NG1 257.10	LG6	Pyrite	5.0x1.2	39.55	31.68	5.81	4.70	0.80	11.80	1.46	1.38	97.19				X	
		Cr PtS	4.3x2.1	36.10	45.44	5.05	3.17	2.28	1.37	nd	nd	93.41	Ti 0.48%	X			
		Cr	2.6x2.2	36.64	51.99	6.24	3.07	1.89	1.32	nd	nd	101.15		X			
		Cr Cpy.	2.9x1.9	37.76	50.75	5.33	2.58	2.03	1.90	nd	nd	100.74		X			
NG1 331.13B	LG5	Cr	2.8x2.1	35.60	49.30	8.09	4.23	3.09	1.56	nd	nd	101.87		X			
		Cr Rut.	2.9x1.8	35.71	49.52	8.07	4.21	3.10	1.57	nd	nd	102.17		X			
NG1 331.65A	LG5	Cr Rut. PtPdS?	3.2x2.4	36.57	48.63	7.11	3.35	2.08	1.85	0.50	nd	98.08	Ti 0.25%	X			
		Cr	4.6x3.7	36.85	52.14	3.69	3.58	1.92	1.01	nd	nd	99.38		X			
		Cr Pt?	5.6x2.3	37.58	50.17	6.72	4.40	1.82	1.46	nd	nd	102.15		X			
		Cr PtPdS	7.1x4.7	36.34	45.03	6.81	4.23	1.34	1.29	0.34	nd	96.38		X			
NG1 429.55B	LG4	Cr	2.8x2.0	35.97	51.83	3.37	4.23	2.24	0.12	nd	0.44	98.19	Pt 2.59%	X			
		Cr	4.2x3.0	36.52	46.85	5.61	4.17	1.86	0.84	nd	nd	97.84		X			
		Cr Mill.	2.7x2.6	32.99	47.04	5.03	3.38	5.43	2.23	nd	nd	96.11		X			
		Cr	2.5x2.3	36.63	52.06	4.10	2.62	2.06	0.94	nd	nd	98.41		X			
		Cr Pent. Mill.	3.1x2.4	37.07	46.42	6.07	4.27	2.03	1.50	0.50	nd	97.85		X			
		Cr	2.5x2.2	36.68	50.68	6.72	3.74	1.85	1.17	0.33	nd	101.37		X			
		Cr	2.7x2.6	36.00	50.16	4.72	4.36	2.35	1.00	nd	nd	98.59		X			
		Cr	3.0x2.5	37.25	54.88	3.90	3.67	2.01	1.20	0.49	nd	103.45		X			
		Cr Mill.	3.0x2.0	36.27	51.90	3.71	2.54	1.95	1.08	0.80	nd	98.25		X			
		Cr	3.9x2.9	36.10	47.77	6.70	4.11	2.65	1.23	nd	nd	98.56		X			
		Cr Pent.	3.4x2.7	36.76	49.44	6.45	4.57	1.82	1.05	0.30	nd	100.38		X			
NG1 475.10A	LG3	Cr PtPd?	3.3x1.6	36.01	48.72	4.25	3.60	2.14	1.80	nd	nd	96.51		X			
		Cr	3.6x2.0	35.57	46.35	4.56	4.79	2.73	2.06	0.34	nd	96.40		X			
NG1 523.95B	LG2a	Cr	3.0x2.7	36.31	45.74	10.25	6.49	2.05	0.61	nd	nd	101.65		X			
		Cr	2.1x2.0	35.57	48.75	4.94	4.75	3.12	1.42	nd	nd	99.56		X			
		Sil.	3.4x3.0	36.32	49.32	5.99	3.86	1.71	0.67	nd	nd	97.87					X
		Sil.	4.6x3.0	36.84	46.15	7.46	4.32	1.68	1.23	nd	nd	97.68					X
		Cr Sil.	2.6x2.2	36.64	47.45	7.84	6.64	1.94	1.21	nd	nd	101.91		X			
NG1 560.10A	LG1	Cr	2.5x2.0	36.76	45.48	7.72	2.98	2.29	1.90	0.35	nd	97.48		X			
		Cr	1.7x1.6	36.12	43.39	10.47	5.92	2.85	2.19	nd	nd	100.93		X			
		Cr Rut.	2.4x1.6	33.82	44.93	6.31	5.35	3.41	1.85	nd	nd	95.68	Ti 0.26%	X			
NG1 609.47	chromite in pyroxenite	Cr Rut. Sil.	6.1x4.1	36.56	46.33	6.68	3.75	1.58	0.68	nd	nd	97.59		X			
		Cr	4.5x4.0	36.92	51.44	5.14	3.71	1.60	0.83	nd	nd	99.63		X			
		Cr	2.7x2.3	35.49	47.48	6.97	2.75	2.62	1.62	nd	nd	96.93		X			
NG1 644.20	chromite in pyroxenite	Cr Rut. Sil.	2.4x2.0	33.38	44.56	8.58	4.17	2.41	1.35	nd	nd	94.44	Ti 0.59%	X			
NG2 158.60	chromite in pyroxenite	Cr PtS	2.9x1.8	32.67	36.27	13.51	6.82	3.02	2.01	nd	nd	94.09	Pt 7.94%	X			
		Cr	1.4x1.1	23.73	29.76	9.48	4.56	10.32	6.96	nd	nd	84.80		X			
NG2 255.88	chromite in pyroxenite	Cr	7.0x5.7	37.77	52.24	7.16	4.14	1.04	0.75	nd	nd	103.09		X			
		Cr	7.0x5.7	37.19	51.44	6.79	3.41	1.02	0.83	nd	nd	100.67		X			
		Cr	2.0x1.1	33.19	47.43	5.98	3.82	3.51	2.07	nd	nd	96.00	Ti 0.37%	X			

Abbreviations: Cr=chromite; Cpy=chalcopyrite; Sil=silicate; Rut=rutile; Spin=spinel; Pent=pentlandite; Mill=millerite
gb=grain boundary; bms=base metal sulphide ; nd=not detected

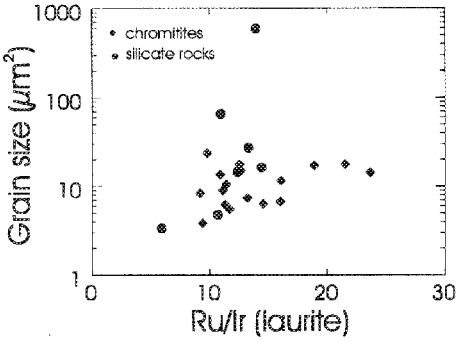

Figure 1 Bivariant plot of grain size *versus* Ru/Ir of laurites.

The number of laurite grains observed varies strongly between individual samples. In two of the samples investigated, (Bastard and Tarentaal chromitite) no laurite was found. Only one laurite grain was found in the top chromitite stringer of the Merensky Reef. This grain is part of a composite inclusion in chromite, consisting of a large chalcopyrite grain hosting the laurite, a Pt-sulphide, a Pt–Fe alloy, and several silicates. No laurite was found in interstitial base-metal sulphides of the Merensky Reef sample investigated, but in a more comprehensive study, Kinloch (1982) observed that 34% by number of the PGM in the Merensky Reef at Union Section is laurite. In four slides from the UG1 and UG2, 42 laurite grains were located (29 in two slides from the UG2 and 13 in two slides from the UG1). In four slides from the MG chromitites, 17 laurite grains were found, and in seven slides from the LG layers, 35 laurite grains were found. In seven slides of chromite-bearing silicate rocks, 48 laurite grains were found. Thus, chromite in some of the silicate rocks appears to be relatively enriched in laurite over chromite in most chromitites, which is notable in view of the generally lower whole-rock Ru contents of the silicate rocks (20 – 30 ppb, Maier and Barnes, unpubl. data) relative to the chromitites (60 – 1100 ppb, Scoon and Teigler, 1994; Von Gruenewaldt and Merkle, 1995). Whether this is purely a nugget effect cannot be assessed as whole-rock PGE contents are not available for the two most laurite-enriched silicate samples (NG1 65.6, NG1 245.4A). Of note is that the bulk Ru content of the massive chromitites exceeds that accounted for by the laurites in our samples by a factor of three to four. For example, laurites observed within the UG2 samples account for approximately 300 ppb Ru, assuming a broadly homogenous distribution of the grains, whereas whole-rock Ru contents of the UG2 are around 1100 ppb (Von Gruenewaldt and Merkle, 1995).

There appears to be no systematic variation in shape or size among laurites included in different hosts. Most grains are euhedral or subhedral, less than 5μm in diameter, and may be hexagonal equant to tabular. In contrast, there is a weak positive correlation between the size and the Ru/Ir ratio of laurite grains (Figure 1). As the size of the observed grains is partly governed by the way they are cut, it cannot be excluded that this pattern reflects compositional zonation of the laurites towards more Ru-rich cores, as has been observed in some of the analysed grains, and also in the Bird River Sill, Canada (Ohnenstetter *et al.*, 1986). Laurites display relatively minor compositional variation with stratigraphic height, both in terms of Ru/Ir and Os/(Os+Ir) ratios (Figure 2). This is in broad accord with the pattern observed in the Stillwater Complex (Talkington and Lipin, 1986). Laurite is plotted within the ternary diagram Ru–Os–Ir in Figure 3, showing that they

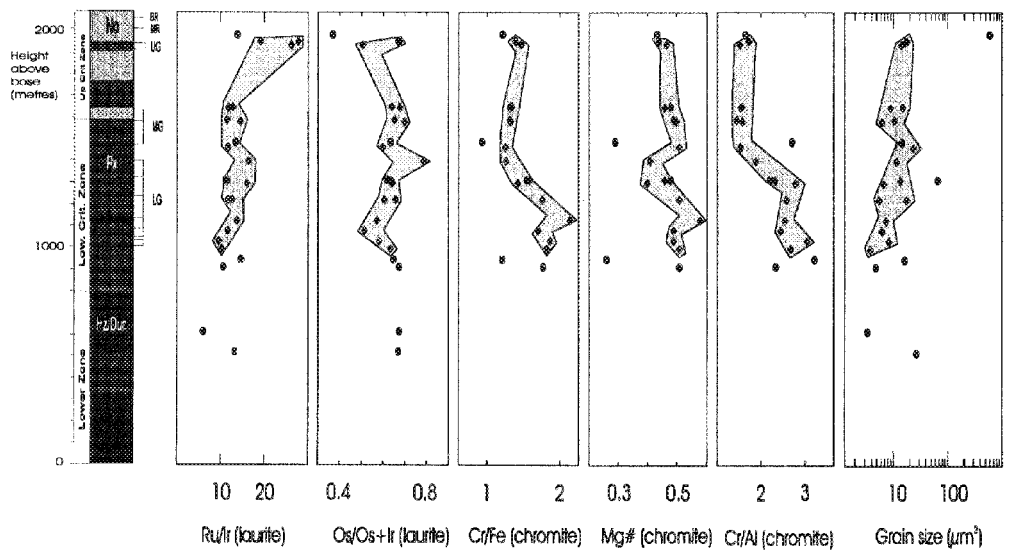

Figure 2 Compositional variation and grain size of laurites as well as Cr/Fe, Mg#, and Cr/Al of chromite hosts plotted *versus* stratigraphic height in a borehole through the Lower and Critical Zones of the Bushveld Complex at Union Section. (Height in metres; Hz — harzburgite, Dun — dunite, Px — pyroxenite, No — norite, MR — Merensky Reef, BR — bastard reef.)

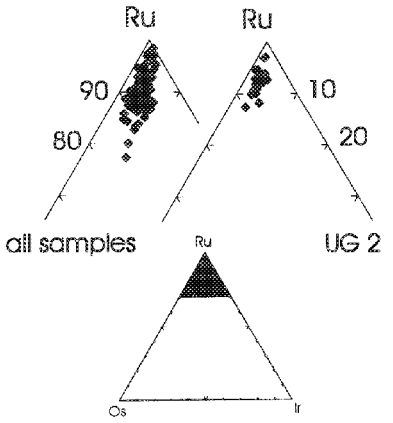

Figure 3 Projection of laurite compositions into the ternary diagram Ru–Os–Ir (atomic per cent).

span a similar compositional range to those in the Stillwater Complex and the Bird River sill. The highest Cr and Fe contents in laurite tend to occur in the smallest grains (Table 1), suggesting that these metal concentrations represent analytical interference from the host chromite. McLaren and De Villiers (1982) found that laurite included in Bushveld chromite is relatively Ru-rich compared to those hosted by silicates and sulphides, but this could not be confirmed by us, possibly due to our limited database.

Discussion

Partitioning of the IPGE into the chromite lattice has been a widely invoked mechanism to explain the close association of laurite with chromite (Grimaldi and Schnepfe, 1969; Agiorgitis and Wolf, 1978; Oshin and Crocket, 1982; Capobianco and Drake, 1990). For example, the relatively chromite-poor Platreef, Merensky Reef, Bastard Reef, and Tarentaal layers all contain little laurite in comparison to the massive chromitites. However, the limited data presented here do not support this mechanism. (i) The correlation between IPGE and chromite contents in the analysed sequence is poor, both within silicate rocks and chromitites (Figure 4). (ii) Chromite within the silicate rocks appears to have higher IPGE tenors than chromite in chromitite, implying that partition coefficients of the IPGE into disseminated chromite would have had to be higher than those into massive chromite, which appears to be unlikely. In fact, some isolated chromite grains in silicate rocks may contain laurite inclusions measuring up to 5% of the size of the chromite host. (iii) The laurite displays considerable compositional variation within individual samples. We consider it unlikely, at present, that this is an alteration effect (*i.e.* Ir or Os loss), since there is no apparent correlation between laurite composition and locality within the chromite host.

It should be noted that the paucity of laurite in the few analysed samples of the chromitite stringers from the Merensky, Bastard, and Tarentaal layers does not necessarily argue against the exsolution model. Firstly, the data of Kinloch (1982) suggest that other Merensky Reef chromite samples may contain significant numbers of laurite grains. Secondly, Nicholson and Mathez (1991) suggested that the Merensky (and Bastard) chromitite stringers are secondary crystallization products of hydrous late-stage melt in which the stability field of chromite is considerably enlarged. Ru (and Ir) would not be able to partition significantly into such late-stage chromite and thus it would not be expected to produce as many exsolved laurites as in primary magmatic chromites.

Some authors have suggested that laurite and other PGM may crystallize directly from the silicate magma to serve as nucleation sites for later crystallizing chromite (Keays and Campbell, 1981; Davies and Tredoux, 1985; Merkle, 1992). However, most workers consider this unlikely, due to the kinetic problems involved in crystallizing a phase that has IPGE in the percentage range from a magma in which the IPGE occur in the low ppb range (Barnes, 1993; Peach and Mathez, 1996). Furthermore, the PGE generally have high solubilities in silicate melts, up to 1000 ppb in the case of Ir (Peach and Mathez, 1996), and thus PGM are unlikely to be stable in silicate magmas.

Crystallization of PGM from sulphide melt in which the PGE have been pre-concentrated, followed by entrainment of the PGM by early crystallizing chromite, has been proposed as a more viable model to crystallize primary PGM (Barnes, 1993). Chromite crystallization and sulphide segregation may both be triggered by magma mixing (Irvine, 1975; 1977), and thus one could perhaps expect chromitite to be enriched in

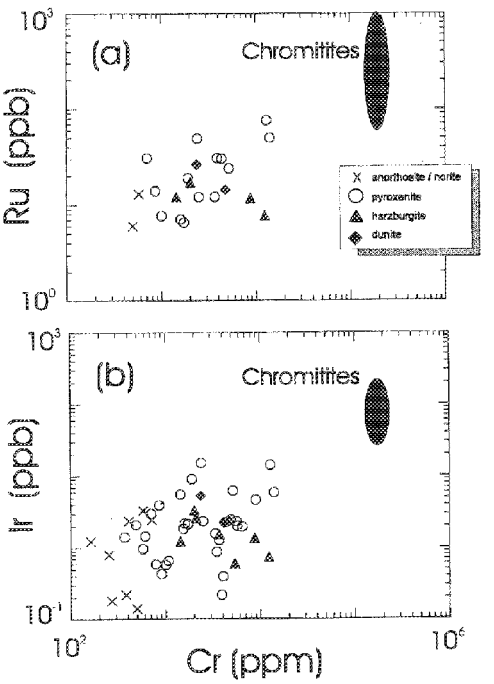

Figure 4 Bivariant diagrams of whole-rock data showing plots of (a) Ru, and (b) Ir versus Cr content. Cr data are corrected for Cr in orthopyroxene, using microprobe analyses and modal data of Teigler and Eales (1996) and De Klerk (1992).

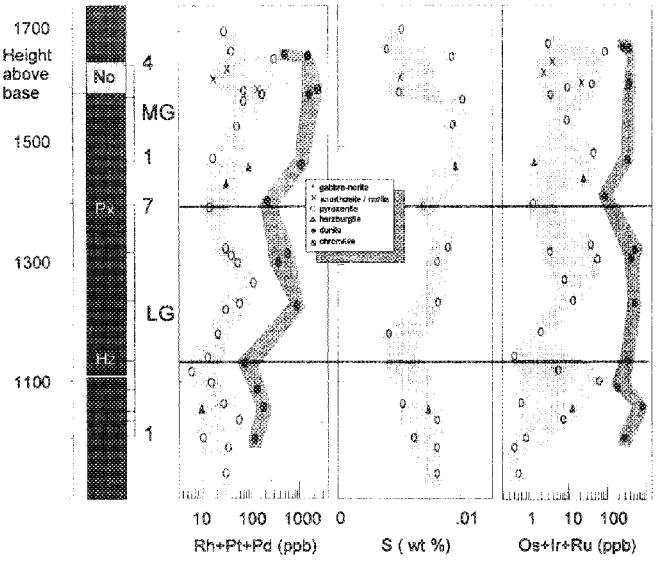

Figure 5 Whole-rock PPGE (Pt+Pd+Rh), IPGE (Os+Ir+Ru), and S contents of rocks in the Upper Critical Zone at Union Section, plotted *versus* stratigraphic height in metres (data from Scoon and Teigler, 1994, and unpublished data of Maier and Barnes).

sulphides and PGE. Crystallization of the laurite grains from sulphide melt may also be supported by the fact that their Ru/Ir ratios are comparable to those of the postulated parental magmas (Davies and Tredoux, 1985), in view of the broadly similar D values of the PGE into sulphide melt. The PPGE and S contents of silicate rocks and chromitites in the Critical Zone show a well-defined positive correlation (Figure 5), suggesting that the PPGE contents are controlled by sulphides. Whether the IPGE within the chromitites show a similar correlation with S cannot be directly established, due to the fact that S contents of most analysed chromitite layers were below the detection limit of 0.01 wt.% (Scoon and Teigler, 1994). However, the IPGE contents of the chromitites show a distinct positive correlation with the PPGE contents, implying that all PGE are governed by the same collector, that is, sulphide melt. The low S contents of the rocks, in particular the chromitites, may be a result of extremely large R-factors during sulphide segregation (Maier *et al.*, 1996) and/or S- and Fe-loss of the sulphides during equilibration with chromite (Naldrett and Lehmann, 1987).

Conclusions

The present study provides a database on the composition of laurite within the Lower and Critical Zones of the western Bushveld Complex at Union Section. We argue that subsolidus exsolution of laurite from the chromite lattice, as well as direct crystallization of laurite from the silicate melt, are unlikely processes in the analysed sequence. Instead, we favour crystallization of laurite from sulphide melt in which the PGE have been preconcentrated, followed by entrapment of the laurites by growing chromite grains. However, quantitative modeling of this process must await experimental data on PGE partitioning between sulphide melt and metal phases.

Acknowledgements

This project was funded by grants from the University of Pretoria (to W.D.M.) and the University of Cardiff (to H.M.P.). The sample material was most helpfully provided by H.V. Eales from Rhodes University, Grahamstown, who obtained it from the Council for Geoscience (NG samples) and AMPLATS (U samples). E. Kinloch and D. Ohnenstetter provided helpful and constructive reviews of the manuscript.

References

Agiorgitis, G. and Wolf, R. (1978). Aspects of osmium, ruthenium and iridium contents in some Greek chromites. *Chem. Geol.*, **23**, 267–272.

Barnes, S.-J., Boyd, R., Korneliussen, A., Nilsson, L.-P., Often, M., Pedersen, R.B. and Robins, B. (1988). The use of mantle normalization and metal ratios in discriminating between the effects of partial melting, crystal fractionation and sulphide segregation on platinum group elements, gold, nickel and copper: examples from Norway. *In:* Pritchard, H.M., Potts, P.J., Bowles, J.F.W. and Cribb, S.J. (Eds.), *Geo Platinum '87*. Elsevier, London, UK, 113–143.

Barnes, S.J. (1993). Partitioning of the platinum group elements and gold between silicate and sulphide magmas in the Munni Munni Complex, Western Australia. *Geochim. Cosmochim. Acta*, **57**, 1277–1290.

Bezmen, N.I., Asif, M., Brügmann, G.E., Romanenko, I.M. and Naldrett, A.J. (1994). Distribution of Pd, Rh, Ru, Ir, Os, and Au between sulfide and silicate metals. *Geochim. Cosmochim. Acta*, **58**, 1251–1260.

Capobianco, C.J. and Drake, M.J. (1990). Partitioning of Ru, Rh, and Pd between spinel and silicate melt and implications for platinum-group element fractionation trends. *Geochim. Cosmochim. Acta*, **54**, 869–874.

Davies, G. and Tredoux, M. (1985). The platinum-group element and gold contents of the marginal rocks and sills of the Bushveld Complex. *Econ. Geol.*, **80**, 838–848.

De Klerk, W.J. (1992). *Petrogenesis of the Upper Critical Zone in the Western Bushveld Complex, with emphasis on the UG1 and Bastard Units.*

Ph.D. thesis (unpubl.), Rhodes University, Grahamstown, S. Afr., 294 pp.
Eales, H.V. and Reynolds, I.M. (1986). Cryptic variations within chromitites of the Upper Critrical Zone, northwestern Bushveld Complex. *Econ. Geol.*, **81**, 1056–1066.
Fleet, M.E., Stone, W.E. and Crocket, J.H. (1991). Partitioning of palladium, iridium, and platinum between sulfide liquid and basalt melt: effects of melt composition, concentration and oxygen fugacity. *Geochim. Cosmochim. Acta*, **55**, 2545–2554.
Grimaldi, F.S. and Schnepfe, M.M. (1969). Mode of occurrence of platinum, palladium, and rhodium in chromitite. *Prof. Pap. US Geol. Surv.*, **650C**, 149–151.
Irvine, T.N. (1975). Crystallization sequences in the Muskox Intrusion and other layered intrusions II: origin of chromitite layers and similar deposits of magmatic ores. *Geochim. Cosmochim. Acta*, **39**, 991–1020.
Irvine, T.N. (1977). Origin of chromitite layers in the Muskox intrusion and other stratiform intrusions II: a new interpretation. *Geology*, **5**, 273–277.
Keays, R.R. and Campbell, I.H. (1981). Precious metals in the Jimberlana Intrusion, Western Australia: Implications for genesis of platiniferous ores in layered intrusions. *Econ. Geol.*, **76**, 1118–1141.
Kinloch, E.D. (1982). Regional trends in the Platinum-group mineralogy of the Critical Zone of the Bushveld Complex, South Africa. *Econ. Geol.*, **77**, 1328–1347.
Maier, W.D., Barnes, S.-J., Teigler, B., De Klerk, W.J. and Mitchell, A.A. (1996). Cu/Pd and Cu/Pt of silicate rocks in the Bushveld Complex: Implications for platinum-group element exploration. *Econ. Geol.*, **91**, 1151–1158.
McLaren, C.H. and De Villiers, J.P.R. (1982). The platinum-group chemistry and mineralogy of the UG2 chromitite layer of the Bushveld Complex. *Econ. Geol.*, **77**, 1348–1366.
Merkle, R.K.W. (1992). Platinum-group minerals in the middle group of chromitite layers at Marikana, western Bushveld Complex: indications for collection mechanisms and postmagmatic modification. *Can. J. Earth Sci.*, **29**, 209–221.
Naldrett, A.J. and Lehmann, J. (1987). Spinel non-stoichiometry as the explanation for Ni-, Cu-, and PGE-enriched sulphides in chromitites. *In*: Pritchard, H.M., Potts, P.J., Bowles, J.F.W. and Cribb, S.J. (Eds.), *Geo Platinum '87*. Elsevier, London, UK, 113–143.
Nicholson, D.M. and Mathez, E.A. (1991). Petrogenesis of the Merensky Reef in the Rustenburg section of the Bushveld Complex. *Contr. Miner. Petrol.*, **107**, 293–309.
Ohnenstetter, D., Watkinson, D.H., Jones, P.C. and Talkington, R. (1986). Cryptic compositional variation in laurite and enclosing chromite from the Bird River Sill, Manitoba. *Econ. Geol.*, **81**, 1159–1168.
Oshin, I.O. and Crocket, J.H. (1982). Noble metals in the Thetford mines ophiolite, Quebec, Canada. Part I: Distribution of gold, iridium, platinum, and palladium in the ultramafic and gabbroic rocks. *Econ. Geol.*, **77**, 1556–1570.
Peach, C.L. and Mathez, E.A. (1996). Constraints on the formation of platinum-group element deposits in igneous rocks. *Econ. Geol.*, **91**, 439–450.
Scoon, R.N. and Teigler, B. (1994). Platinum-group element mineralization in the Critical Zone of the Western Bushveld Complex: I. Sulfide poor chromitites below the UG2. *Econ. Geol.*, **89**, 1094–1121.
Stone, W.E., Crocket, J.H. and Fleet, M.E. (1990). Partitioning of palladium, iridium, platinum and gold between sulfide liquid and basalt melt at 1200 °C. *Geochim. Cosmochim. Acta*, **54**, 2341–2344.
Talkington, R.W. and Lipin, B.R. (1986). Platinum-group minerals in chromite seams of the Stillwater Complex, Montana. *Econ. Geol.*, **81**, 1179–1186.
Teigler, B. and Eales, H.V. (1996). The Lower and Critical Zones of the western limb of the Bushveld Complex as intersected by the Nooitgedacht boreholes. *Bull. Geol. Surv. S. Afr.*, **111**, 126 pp.
Von Gruenewaldt, G. and Merkle, R.K.W. (1995). Platinum group element proportions in chromitites of the Bushveld Complex: implications for fractionation and magma mixing models. *J. Afr. Earth Sci.*, **21**, 615–632.

Editorial handling: R.G. Cawthorn.